

Pre-buckling responses of Timoshenko nanobeams based on the integral and differential models of nonlocal elasticity: an isogeometric approach

A. Norouzzadeh¹ · R. Ansari¹ · H. Rouhi²

Received: 13 December 2016 / Accepted: 3 March 2017 / Published online: 9 April 2017
© Springer-Verlag Berlin Heidelberg 2017

Abstract Differential form of Eringen's nonlocal elasticity theory is widely employed to capture the small-scale effects on the behavior of nanostructures. However, paradoxical results are obtained via the differential nonlocal constitutive relations in some cases such as in the vibration and bending analysis of cantilevers, and recourse must be made to the integral (original) form of Eringen's theory. Motivated by this consideration, a novel nonlocal formulation is developed herein based on the original formulation of Eringen's theory to study the buckling behavior of nanobeams. The governing equations are derived according to the Timoshenko beam theory, and are represented in a suitable vector–matrix form which is applicable to the finite-element analysis. In addition, an isogeometric analysis (IGA) is conducted for the solution of buckling problem. Construction of exact geometry using non-uniform rational B-splines and easy implementation of geometry refinement tools are the main advantages of IGA. A comparison study is performed between the predictions of integral and differential nonlocal models for nanobeams under different kinds of end conditions.

1 Introduction

Continuum mechanics-based models are extensively applied for the mechanical analysis of micro- and nanostructures largely owing to their computational effectiveness in comparison with the available atomistic approaches such as molecular dynamics simulations and quantum mechanics-based methods. As the classical continuum mechanics is scale-free and cannot capture the small-scale influences, several higher order continuum theories have been developed that are able to detect the size-dependent behavior of micro- and nanostructures. The surface elasticity theory [1–7], strain gradient theory [8–10], and couple stress theory [11–14] are examples of such theories.

The nonlocal elasticity theory is another higher order continuum theory which is growing in popularity. The concept of nonlocality is inherent in solid-state physics where the nonlocal attractions of atoms are dominant. Based upon the classical continuum mechanics, the stress tensor at a reference point of a body can be obtained using the strain tensor at that point. However, according to the nonlocal continuum mechanics, the stress tensor at a reference point in a body depends not only on the strain tensor at that point, but also on the strain tensor at all other points of the body. The linear nonlocal elasticity theory was primarily proposed by Kröner [15], Krumhansl [16] and Kunin [17], and then developed by Eringen [18] and Eringen and Edelen [19]. The nonlocal elasticity theory has been originally formulated in the integral form in which kernel functions are used for considering nonlocal effects [18, 19]. In 1983, Eringen [20] proposed the differential version of the nonlocal theory with considering a specific kernel function (Green function of linear differential operator). Since dealing with the differential nonlocal constitutive equations is simpler than dealing with their integral counterparts, a lot

✉ R. Ansari
r_ansari@guilan.ac.ir

¹ Department of Mechanical Engineering, University of Guilan, 3756, Rasht, Iran

² Department of Engineering Science, Faculty of Technology and Engineering, East of Guilan, University of Guilan, 44891-63157 Rudsar-Vajargah, Iran

of research works can be found in which the differential form of nonlocal theory has been employed to capture the nonlocal effects. In particular, several differential nonlocal beam, plate, and shell models have been developed for the problems of nanobeams [21–24], nanotubes [25–29], and nanoplates [30–35].

The reliability of Eringen's differential nonlocal model has been proved in various problems. For example, in [29, 33, 36–38], it was revealed that the accuracy of the results of such model is comparable to that of molecular dynamics simulations provided that the nonlocal parameter is suitably adjusted. However, one can show that using the differential nonlocal model leads to inconsistent results in some specific cases. A well-known paradox happens when this model is used for computing natural frequencies and deflections of cantilevers. It is generally accepted that the stiffness of structure decreases by increasing the nonlocal parameter. Surprisingly, increasing the nonlocal parameter has a stiffening influence on the behavior of cantilevers [39, 40]. Therefore, some attempts have been made in recent years, for example by Polizzotto [41], Pisano and Fuschi [42], Challamel et al. [43, 44], Khodabakhshi and Reddy [45], Fernández-Sáez et al. [46], and Norouzzadeh and Ansari [47] to resolve such paradoxes using Eringen's integral nonlocal model.

The isogeometric analysis (IGA) [48, 49] is a new numerical method whose source of inspiration comes from the finite-element method (FEM) and the computer-aided design (CAD). Construction of exact geometry using non-uniform rational B-splines (NURBS) and easy implementation of geometry refinement tools are the key advantages of IGA. There are also several powerful numerical solution strategies, like discrete singular convolution (DSC) and differential quadrature (DQ) methods, which have attracted attention of researchers in recent years. For example, one can mention the paper of Ersoy et al. [50] in which DSC and DQ are utilized to determine the fundamental frequencies of different shells and annular plates. In addition, Civalek [51] studied the free vibration behavior of rotating shells based on the DSC method. He examined the influences of using different materials including isotropic, orthotropic, functionally graded and laminated ones on the frequencies of truncated conical shells, circular shells, and panels.

In the present paper, based on integral formulation of nonlocal elasticity theory, the stability characteristics of nanobeams under the action of axial load are investigated. First, the governing equations are derived using Eringen's integral model together with the Timoshenko beam theory. The equations are obtained in the vector–matrix form which is suitable for the finite-element-based analyses. In the next step, an isogeometric analysis is conducted so as to study the buckling response of nanobeams with various types of boundary

conditions. In addition, the governing equations are derived and solved based on Eringen's differential model for the comparison purpose. Selected numerical results are presented on the buckling of nanobeams using integral and differential nonlocal models as well as the local (classical) model.

2 Integral formulation of Eringen's nonlocal model

2.1 Governing equations

Consider a nanobeam with geometrical parameters as length L , width b , and thickness h . According to the integral formulation of Eringen's nonlocal model [18, 19], the constitutive equations of beam-type structures are presented in following form:

$$t_{ij}(x, x_3) = \lambda \delta_{ij} \varepsilon_{kk}(x, x_3) + 2\mu \varepsilon_{ij}(x, x_3) = C_{ijkl} \varepsilon_{kl}(x, x_3), \quad (1)$$

$$\sigma_{ij}(\bar{x}, x_3) = \int_x k(|x - \bar{x}|, \kappa) t_{ij}(x, x_3) dx + \delta_{ij} \sigma_0. \quad (2)$$

In these relations, t_{ij} , σ_{ij} , and ε_{ij} are the local and nonlocal stresses and strain tensors, respectively. In addition, σ_0 shows the initial stress and C_{ijkl} denotes the elasticity tensor. Besides, Lamé's constants are given by

$$\lambda = E\nu / (1 - \nu^2), \quad \mu = E / (2(1 + \nu)). \quad (3)$$

The stress field at reference point $\bar{x} = \bar{x}_1$ is a function of strains of all points on domain $x = x_1$. Moreover, k is the kernel function which is determined in terms of nonlocal parameter κ and neighborhood distance $|x - \bar{x}|$.

The strain energy of nanobeam can be written as follows:

$$\begin{aligned} \Pi_s &= \frac{1}{2} \int_A \int_{\bar{x}} \sigma_{ij}(\bar{x}, x_3) \varepsilon_{ij}(\bar{x}, x_3) d\bar{x} dA \\ &= \frac{1}{2} \int_A \int_{\bar{x}} \left(\int_x k(|x - \bar{x}|, \kappa) t_{ij}(x, x_3) dx + \delta_{ij} \sigma_0 \right) \varepsilon_{ij}(\bar{x}, x_3) d\bar{x} dA, \end{aligned} \quad (4)$$

and the variation form of this energy is determined as follows:

$$\begin{aligned} \delta \Pi_s &= \int_A \int_{\bar{x}} \sigma_{ij}(\bar{x}, x_3) \delta \varepsilon_{ij}(\bar{x}, x_3) d\bar{x} dA \\ &= \int_A \int_{\bar{x}} \left(\int_x k(|x - \bar{x}|, \kappa) t_{ij}(x, x_3) dx + \delta_{ij} \sigma_0 \right) \delta \varepsilon_{ij}(\bar{x}, x_3) d\bar{x} dA. \end{aligned} \quad (5)$$

The nanobeam is modelled by the Timoshenko beam theory. Displacement field components are thus given by

$$u_1(x, x_3) = u(x) + x_3 \psi(x), \quad u_3(x, x_3) = w(x), \quad (6)$$

whose matrix–vector forms are presented as

$$\mathbf{u}(x, x_3) = \mathbf{P}_1(x_3)\mathbf{q}(x), \mathbf{u}(x, x_3) = [u_1 \ u_3]^T$$

$$\mathbf{P}_1(x_3) = \begin{bmatrix} 1 & 0 & x_3 \\ 0 & 1 & 0 \end{bmatrix}, \mathbf{q}(x) = [u \ w \ \psi]^T, \tag{7}$$

where u , w , and ψ are the axial and transverse displacements, and the rotation angle of the cross section with respect to the vertical direction, respectively.

Therefore, the constitutive equations can be written as follows:

$$\bar{\boldsymbol{\sigma}}(\bar{x}, x_3) = \int_x k(|x - \bar{x}|, \kappa) \mathbf{C} \boldsymbol{\varepsilon}(x, x_3) \, dx + \boldsymbol{\sigma}_0, \tag{8}$$

$$\bar{\boldsymbol{\sigma}}(\bar{x}, x_3) = \begin{bmatrix} \sigma_{xx}(\bar{x}, x_3) \\ \sigma_{xz}(\bar{x}, x_3) \end{bmatrix}, \mathbf{C} = \begin{bmatrix} \lambda + 2\mu & 0 \\ 0 & k_s \mu \end{bmatrix}, \tag{9}$$

$$\boldsymbol{\varepsilon}(x, x_3) = \begin{bmatrix} \varepsilon_{xx}(x, x_3) \\ 2\varepsilon_{xz}(x, x_3) \end{bmatrix}, \boldsymbol{\sigma}_0 = \begin{bmatrix} \sigma_0 \\ 0 \end{bmatrix},$$

in which $\bar{\boldsymbol{\sigma}}$, $\boldsymbol{\varepsilon}$, and \mathbf{C} are the stress vector at reference point, strain vector, and elastic matrix, respectively. Furthermore, $k_s = 5/6$ stands for the shear correction factor and $\boldsymbol{\sigma}_0$ is the initial stress vector.

The strain–displacement relation is considered as

$$\varepsilon_{ij} = \frac{1}{2} \left(\frac{\partial u_i}{\partial x_j} + \frac{\partial u_j}{\partial x_i} \right), \tag{10}$$

which can be expressed in the following matrix–vector form:

$$\boldsymbol{\varepsilon}(x, x_3) = \left(\mathbf{P}_1(x_3)\mathbf{E}_l + \frac{1}{2}\mathbf{P}_2(x_3)\mathbf{E}_n \right) \mathbf{q}(x), \tag{11}$$

$$\mathbf{P}_2(x_3) = \begin{bmatrix} 1 \\ 0 \end{bmatrix}, \tag{12}$$

$$\mathbf{E}_l = \begin{bmatrix} \partial/\partial x & 0 & 0 \\ 0 & \partial/\partial x & 1 \\ 0 & 0 & \partial/\partial x \end{bmatrix}, \tag{13}$$

$$\mathbf{E}_n = (\mathbf{G}\mathbf{q})\mathbf{G}, \mathbf{G} = [0 \ \partial/\partial x \ 0]. \tag{14}$$

Using the obtained equations so far, one can achieve the following relations of strain energy and its variation:

$$\Pi_s = \frac{1}{2} \int_A \int_{\bar{x}} \bar{\boldsymbol{\varepsilon}}^T(\bar{x}, x_3) \bar{\boldsymbol{\sigma}}(\bar{x}, x_3) \, d\bar{x} dA, \tag{15}$$

$$\delta \Pi_s = \int_A \int_{\bar{x}} \delta \bar{\boldsymbol{\varepsilon}}^T(\bar{x}, x_3) \bar{\boldsymbol{\sigma}}(\bar{x}, x_3) \, d\bar{x} dA, \tag{16}$$

in which the strain vector at reference point $\bar{\boldsymbol{\varepsilon}}$ is determined by substituting x to \bar{x} ($x \rightarrow \bar{x}$) in Eqs. (11), (13), and Eq. (14), i.e.,

$$\bar{\mathbf{E}}_l = \mathbf{E}_l|x \rightarrow \bar{x}, \bar{\mathbf{E}}_n = \mathbf{E}_n|x \rightarrow \bar{x}, \bar{\mathbf{q}} = \mathbf{q}|x \rightarrow \bar{x}. \tag{17}$$

Accordingly, the final form of stress vector and strain energy terms is obtained as follows:

$$\bar{\boldsymbol{\sigma}}(\bar{x}, x_3) = \int_x k(|x - \bar{x}|, \kappa) \mathbf{C} \left(\mathbf{P}_1 \mathbf{E}_l + \frac{1}{2} \mathbf{P}_2 \mathbf{E}_n \right) \mathbf{q} \, dx + \boldsymbol{\sigma}_0, \tag{18}$$

$$\Pi_s = \frac{1}{2} \int_{\bar{x}} \bar{\mathbf{q}}^T \left[\bar{\mathbf{E}}_l^T \left(\int_x k \left(\bar{\mathbf{C}}_{11} \mathbf{E}_l + \frac{1}{2} \bar{\mathbf{C}}_{12} \mathbf{E}_n \right) \mathbf{q} \, dx + \mathbf{N}_1 \right) + \frac{1}{2} \bar{\mathbf{E}}_n^T \left(\int_x k \left(\bar{\mathbf{C}}_{21} \mathbf{E}_l + \frac{1}{2} \bar{\mathbf{C}}_{22} \mathbf{E}_n \right) \mathbf{q} \, dx + \mathbf{N}_2 \right) \right] d\bar{x}, \tag{19}$$

$$\delta \Pi_s = \int_{\bar{x}} \delta \bar{\mathbf{q}}^T \left[\bar{\mathbf{E}}_l^T \left(\int_x k \left(\bar{\mathbf{C}}_{11} \mathbf{E}_l + \frac{1}{2} \bar{\mathbf{C}}_{12} \mathbf{E}_n \right) \mathbf{q} \, dx + \mathbf{N}_1 \right) + \bar{\mathbf{E}}_n^T \left(\int_x k \left(\bar{\mathbf{C}}_{21} \mathbf{E}_l + \frac{1}{2} \bar{\mathbf{C}}_{22} \mathbf{E}_n \right) \mathbf{q} \, dx + \mathbf{N}_2 \right) \right] d\bar{x} \tag{20}$$

where

$$\bar{\mathbf{C}}_{ij} = \int_A \mathbf{P}_i^T \mathbf{C} \mathbf{P}_j \, dA, \mathbf{N}_i = \int_A \mathbf{P}_i^T \boldsymbol{\sigma}_0 \, dA, i, j = 1, 2, \tag{21}$$

in which

$$\mathbf{N}_1 = N_0 \tilde{\mathbf{N}}, \mathbf{N}_2 = N_0, \tilde{\mathbf{N}} = [1 \ 0 \ 0]^T, N_0 = \int_A \sigma_0 \, dA. \tag{22}$$

2.2 Isogeometric analysis

Based on the integral nonlocal constitutive equations, the stress vector at reference point \bar{x} is determined by integration in domain x . From the viewpoint of IGA, it is required to assemble (in x coordinate) the total stress vector in each point (in \bar{x} coordinate) of Gauss quadrature scheme. Accordingly, the assemblage process should be performed in a two-step manner to achieve the strain energy of body. IGA is able to overcome the difficulty of significant run time with representing the convenient solution properties, like generating unified geometry in a patch and implementing the efficient refinement approaches. In the following, the local coordinate system corresponding to x and \bar{x} determined in terms of control is considered to be ξ and $\bar{\xi}$, respectively.

The nanobeam is modelled herein by one patch. Displacement field can be interpolated by NURBS basis functions as

$$\mathbf{q} = \mathbf{N}(\xi)\mathbf{d}, \bar{\mathbf{q}} = \bar{\mathbf{N}}(\bar{\xi})\bar{\mathbf{d}}, \tag{23}$$

$$\begin{aligned} \mathbf{N}(\xi) &= \mathbf{I}_3 \otimes \hat{\mathbf{N}}(\xi), \hat{\mathbf{N}}(\xi) = [N_1(\xi) \dots N_n(\xi)] \\ \bar{\mathbf{N}}(\bar{\xi}) &= \mathbf{I}_3 \otimes \hat{\bar{\mathbf{N}}}(\bar{\xi}), \hat{\bar{\mathbf{N}}}(\bar{\xi}) = [N_1(\bar{\xi}) \dots N_n(\bar{\xi})] \end{aligned} \tag{24}$$

where N_i denotes the basis function of i th knot and \otimes signals the Kronecker delta product. In addition, \mathbf{d} and $\bar{\mathbf{d}}$ are the control variables in ξ and $\bar{\xi}$ coordinates, respectively.

By inserting Eq. (23) into (11), one has the strain vector of the element as

$$\begin{aligned} \boldsymbol{\varepsilon}(\xi) &= \left(\mathbf{P}_1 \mathbf{B}_l + \frac{1}{2} \mathbf{P}_2 \mathbf{B}_n \right) \mathbf{d}, \bar{\boldsymbol{\varepsilon}}(\bar{\xi}) = \left(\mathbf{P}_1 \bar{\mathbf{B}}_l + \frac{1}{2} \mathbf{P}_2 \bar{\mathbf{B}}_n \right) \bar{\mathbf{d}}, \\ \delta \bar{\boldsymbol{\varepsilon}}(\bar{\xi}) &= (\mathbf{P}_1 \bar{\mathbf{B}}_l + \mathbf{P}_2 \bar{\mathbf{B}}_n) \delta \bar{\mathbf{d}}, \end{aligned} \tag{25}$$

$$\begin{aligned} \mathbf{B}(\xi) &= \mathbf{E}_l \mathbf{N}(\xi), \bar{\mathbf{B}}_l(\bar{\xi}) = \bar{\mathbf{E}}_l \bar{\mathbf{N}}(\bar{\xi}) \\ \mathbf{B}_n(\xi) &= (\mathbf{Q}\mathbf{d})\mathbf{Q}, \mathbf{Q}(\xi) = \mathbf{G}\mathbf{N}(\xi), \bar{\mathbf{B}}_n(\bar{\xi}) = (\bar{\mathbf{Q}}\bar{\mathbf{d}})\bar{\mathbf{Q}}, \bar{\mathbf{Q}}(\bar{\xi}) = \bar{\mathbf{G}}\bar{\mathbf{N}}(\bar{\xi}). \end{aligned} \tag{26}$$

Besides, the stress resultant vector used in Eqs. (19) and (20) is obtained as

$$\begin{aligned} \bar{\boldsymbol{\sigma}}_{i,l} &= \bar{\mathbf{S}}_{i,l} \mathbf{d}, \bar{\boldsymbol{\sigma}}_{i,n} = \frac{1}{2} \bar{\mathbf{S}}_{i,n} \mathbf{d} \\ \bar{\mathbf{S}}_{i,l} &= \int_{\xi} k \bar{\mathbf{C}}_{il} \mathbf{B}_l J d\xi, \bar{\mathbf{S}}_{i,n} = \int_{\xi} k \bar{\mathbf{C}}_{i2} \mathbf{B}_n J d\xi, i = 1, 2, \end{aligned} \tag{27}$$

where J is the Jacobian in ξ coordinate.

Now, the assemblage process in ξ direction is performed which leads to

$$\bar{\mathbf{S}}_{i,l} \rightarrow \bar{\mathbf{S}}_{i,l}, \bar{\mathbf{S}}_{i,n} \rightarrow \bar{\mathbf{S}}_{i,n}, \mathbf{d} \rightarrow \mathbb{d} \tag{28}$$

Consequently, the strain energy of a patch and its variation are determined in terms of control variables as

$$\begin{aligned} \Pi_{s,p} &= \frac{1}{2} \int_{\xi} \bar{\mathbf{d}} \left[\bar{\mathbf{B}}_l^T \left(\left(\bar{\mathbf{S}}_{1,l} \mathbb{d} + \frac{1}{2} \bar{\mathbf{S}}_{1,n} \right) + \mathbf{N}_1 \right) \right. \\ &\quad \left. + \frac{1}{2} \bar{\mathbf{B}}_n^T \left(\left(\bar{\mathbf{S}}_{2,l} + \frac{1}{2} \bar{\mathbf{S}}_{2,n} \right) \mathbb{d} + \mathbf{N}_2 \right) \right] J d\xi \end{aligned} \tag{29}$$

$$\begin{aligned} \delta \Pi_{s,p} &= \int_{\bar{\xi}} \delta \bar{\mathbf{d}}^T \left[\bar{\mathbf{B}}_l^T \left(\left(\bar{\mathbf{S}}_{1,l} + \frac{1}{2} \bar{\mathbf{S}}_{1,n} \right) + \mathbb{d} \mathbf{N}_1 \right) \right. \\ &\quad \left. + \bar{\mathbf{B}}_n^T \left(\left(\bar{\mathbf{S}}_{2,l} + \frac{1}{2} \bar{\mathbf{S}}_{2,n} \right) \mathbb{d} + \mathbf{N}_2 \right) \right] J d\bar{\xi} \\ &= \delta \bar{\mathbf{d}}^T \mathbf{K}_{s,p} \mathbb{d} + \delta \bar{\mathbf{d}}^T \mathbf{N}_{s,p}, \end{aligned} \tag{30}$$

where $\mathbf{K}_{s,p}$ denotes the stiffness matrix given by

$$\begin{aligned} \mathbf{K}_{s,p} &= \mathbf{K}_{s,p}^l + \mathbf{K}_{s,p}^n \\ \mathbf{K}_{s,p}^l &= \int_{\bar{\xi}} \bar{\mathbf{B}}_l^T \bar{\mathbf{S}}_{1,l} J d\bar{\xi} \\ \mathbf{K}_{s,p}^n &= \int_{\bar{\xi}} \left(\frac{1}{2} \bar{\mathbf{B}}_l^T \bar{\mathbf{S}}_{1,n} + \bar{\mathbf{B}}_n^T \bar{\mathbf{S}}_{2,l} + \frac{1}{2} \bar{\mathbf{B}}_n^T \bar{\mathbf{S}}_{2,n} \right) J d\bar{\xi}. \end{aligned} \tag{31}$$

In addition, by considering $\int_{\bar{\xi}} \bar{\mathbf{B}}_l^T \mathbf{N}_1 J d\bar{\xi} = 0$ and $\mathbf{N}_2 = N_0$, the in-plane load $\mathbf{N}_{s,p}$ can be expressed as follows:

$$\mathbf{N}_{s,p} = N_0 \int_{\bar{\xi}} \bar{\mathbf{B}}_n^T J d\bar{\xi} = N_0 \int_{\bar{\xi}} \bar{\mathbf{Q}}^T \bar{\mathbf{Q}} \bar{\mathbf{d}} J d\bar{\xi}. \tag{32}$$

Therefore, the geometric stiffness matrix $\mathbf{K}_{g,p}$ is achieved as follows:

$$\begin{aligned} \delta \bar{\mathbf{d}}^T \mathbf{N}_{s,p} &= N_0 \delta \bar{\mathbf{d}}^T \mathbf{K}_{g,p} \bar{\mathbf{d}} \\ \mathbf{K}_{g,p} &= \int_{\bar{\xi}} \bar{\mathbf{Q}}^T \bar{\mathbf{Q}} J d\bar{\xi}. \end{aligned} \tag{33}$$

Finally

$$\delta \bar{\mathbf{d}}^T (\mathbf{K}_{s,p} \mathbb{d} + N_0 \mathbf{K}_{g,p} \bar{\mathbf{d}}). \tag{34}$$

By performing the assemblage procedure in $\bar{\xi}$ coordinate, one can arrive at

$$\bar{\mathbf{d}} \rightarrow \bar{\mathbb{d}}, \mathbf{K}_{s,p} \rightarrow \mathbb{K}_s, \mathbf{K}_{g,p} \rightarrow \mathbb{K}_g. \tag{35}$$

If the same local coordinate systems are considered in the analysis, one has $\mathbb{d} = \bar{\mathbb{d}}$ and

$$(\mathbb{K}_s + N_0 \mathbb{K}_g) \mathbb{d} = 0. \tag{36}$$

From the presented solution strategy, one can find that the two-step procedure demands higher computational cost than the classical one. For instance, if m times function evaluation is needed in the conventional problem, it turns to m^2 times in the present model.

3 Differential formulation of Eringen’s nonlocal model

3.1 Governing equations

Eringen [20] proposed the differential form of nonlocal constitutive equations as

$$(1 - \kappa^2 \nabla^2) \boldsymbol{\sigma}_{ij} = \lambda \delta_{ij} \boldsymbol{\varepsilon}_{kk} + 2\mu \boldsymbol{\varepsilon}_{ij} = C_{ijkl} \boldsymbol{\varepsilon}_{kl}, \tag{37}$$

$$(1 - \kappa^2 \nabla^2) \boldsymbol{\sigma} = \mathbf{C} \boldsymbol{\varepsilon}, \tag{38}$$

where $\nabla^2 = \partial^2 / \partial x^2$. Here, it is observed that the differential model can be simply reduced to classical elasticity by setting $\kappa = 0$. However, such a manipulation in the original integral model leads to singularity of kernel function.

By neglecting von-Karman nonlinearities, the strain vector is expressed as

$$\boldsymbol{\varepsilon} = \mathbf{P}_1 \mathbf{E}_l \mathbf{q}. \tag{39}$$

The resultant is also defined as

$$\tilde{\mathbf{N}} = \int_A \mathbf{P}_1^T \boldsymbol{\sigma} dA, \tag{40}$$

$$(1 - \kappa^2 \nabla^2) \tilde{\mathbf{N}} = \tilde{\mathbf{C}}_{11} \mathbf{E}_l \mathbf{q}. \tag{41}$$

The strain energy and its variation can be written as

$$\begin{aligned} \Pi_s &= \frac{1}{2} \int_A \int_x \boldsymbol{\varepsilon}^T \boldsymbol{\sigma} dx dA = \frac{1}{2} \int_A \int_x \mathbf{q}^T \mathbf{E}_l^T \mathbf{P}_1^T \boldsymbol{\sigma} dx dA \\ &= \frac{1}{2} \int_x \mathbf{q}^T \mathbf{E}_l^T \tilde{\mathbf{N}} dx, \end{aligned} \tag{42}$$

$$\delta \Pi_s = \int_{x_1}^{x_2} \int_x \delta \mathbf{q}^T \mathbf{E}_l^T \tilde{\mathbf{N}} dx dt. \tag{43}$$

In addition, for the work done by in-plane load, one can write

$$\begin{aligned} \Pi_p &= \frac{1}{2} \int_x N_0 \left(\frac{\partial w}{\partial x} \right)^2 = \frac{1}{2} N_0 \int_x \mathbf{T} dx \\ \boldsymbol{\varepsilon} &= \mathbf{G} \mathbf{q}. \end{aligned} \tag{44}$$

Thus

$$\delta \Pi_p = N_0 \int_x \delta \boldsymbol{\varepsilon}^T \boldsymbol{\varepsilon} dx = N_0 \int_x \delta \mathbf{q}^T \mathbf{G}^T \mathbf{G} \mathbf{q} dx. \tag{45}$$

The variational governing equation is derived as

$$\int_x (\delta \mathbf{q}^T \mathbf{E}_l^T \tilde{\mathbf{N}} + N_0 \delta \mathbf{q}^T \mathbf{G}^T \mathbf{G} \mathbf{q}) dx = \int_x (\delta \mathbf{q}^T \mathbf{E}_l^T \tilde{\mathbf{C}}_{11} \mathbf{E}_l \mathbf{q} + N_0 \delta \mathbf{q}^T \mathbf{G}^T \mathbf{G} (1 - \kappa^2 \nabla^2) \mathbf{q}) dx = 0. \tag{46}$$

Subsequently, one can find the variations of equivalent energy terms as

$$\delta \Pi_s = \int_x \delta \mathbf{q}^T \mathbf{E}_l^T \tilde{\mathbf{C}}_{11} \mathbf{E}_l \mathbf{q} dx, \tag{47}$$

$$\delta \Pi_p = N_0 \int_x \delta \mathbf{q}^T \mathbf{G}^T \mathbf{G} (1 - \kappa^2 \nabla^2) \mathbf{q} dx. \tag{48}$$

3.2 Isogeometric analysis

For the differential nonlocal model, a one-step assemblage procedure can be used in the isogeometric analysis to obtain the governing equations. By adopting the interpolation of displacement field

$$\mathbf{q} = \mathbf{N} \mathbf{d}, \tag{49}$$

$$\mathbf{N} = \mathbf{I}_3 \otimes \hat{\mathbf{N}}, \hat{\mathbf{N}} = [N_1 \dots N_n], \tag{50}$$

one has

$$\boldsymbol{\varepsilon} = \mathbf{P}_1 \mathbf{B}_l \mathbf{d}, \mathbf{B} = \mathbf{E}_l \mathbf{N}. \tag{51}$$

The equivalent energy terms, introduced in Eqs. (47) and (48), are rewritten for a patch as

$$\delta \Pi_{s,p} = \delta \mathbf{d}^T \mathbf{K}_{s,p} \mathbf{d}, \tag{52}$$

$$\delta \Pi_{p,p} = N_0 \delta \mathbf{d}^T \mathbf{K}_{g,p} \mathbf{d}. \tag{53}$$

In addition, the stiffness matrices are

$$\mathbf{K}_{s,p} = \int_{\xi} \mathbf{B}_l^T \tilde{\mathbf{C}}_{11} \mathbf{B}_l J d\xi, \tag{54}$$

$$\mathbf{K}_{g,p} = \int_{\xi} \mathbf{Q}^T \mathbf{Q}_h J d\xi, \mathbf{Q}_h = \mathbf{G} (1 - \kappa^2 \nabla^2) \mathbf{N}. \tag{55}$$

Therefore

$$(\mathbf{K}_{s,p} + N_0 \mathbf{K}_{g,p}) \mathbf{d} = 0, \tag{56}$$

and after assemblage, one has

$$(\mathbb{K}_s + N_0 \mathbb{K}_g) \mathbf{d} = 0. \tag{57}$$

Therefore, in addition to determination of high-order geometric stiffness matrix, there is no difference between the isogeometric analysis of a differential model of nonlocal continuum and that of a classical elasticity. In addition, the straightforward degree elevation characteristic of IGA leads

to easily evaluate the higher order derivative of basis functions in Eq. (55).

4 Numerical results

In this section, the critical buckling loads of Timoshenko nanobeams with clamped-free, clamped-simply supported, and clamped-clamped boundary conditions are obtained using IGA and based on different models. The length-to-thickness and Poisson's ratio of nanobeams are taken as 12 and 0.35, respectively. The dimensionless critical buckling load is also introduced as

$$P_{cr} = N_0 L^2 / D, \tag{58}$$

where $D = \frac{1}{12} E b h^3$. Moreover, the following one-dimensional kernel function is considered:

$$k(|x|, \kappa) = \frac{1}{2\kappa} e^{-|x|/\kappa}. \tag{59}$$

First, it is required to assess the convergence characteristics and validity of the proposed approach. In this regard,

the convergence of IGA is shown in Fig. 1, and a comparison study with the open literature is presented in Table 1. In both cases, the end conditions are considered to be clamped-free.

Variations of non-dimensional critical buckling load of nanobeam with the number of knots (n) are demonstrated in Fig. 1. It is assumed that thickness is $h = 1\text{ nm}$ and the non-local parameter has three different values. In addition, order of basis functions is set as $p = 2$ in the isogeometric analysis of integral model. Because of high-order derivatives in the geometric stiffness matrix, it is considered to be $p = 3$ in

the differential model. As it is expected, one can observe that there is a higher computational requirement in the integral model. Moreover, due to the short range of neighborhood distance in small values of nonlocal parameter, higher number of knots is needed to achieve the convergence [47]. To give a numerical sense of convergence behavior, the following criterion is utilized:

$$\text{Error} = \frac{P_{cr}|_{n=28} - P_{cr}|_{n=26}}{P_{cr}|_{n=10}}$$

Fig. 1 Converging trend of IGA for a clamped-free nanobeam

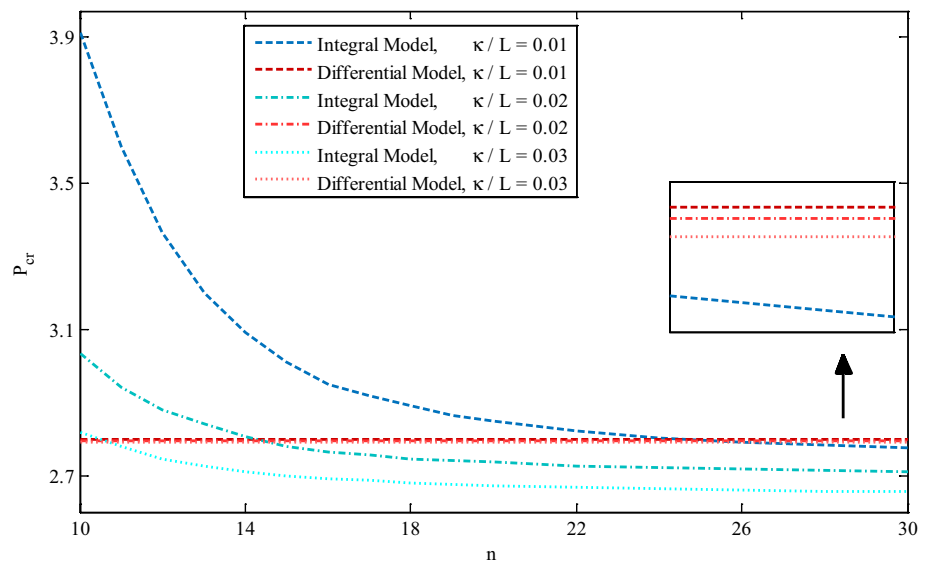


Table 1 Critical buckling loads (nN) of clamped-free nano-rod for various length-to-diameter ratios and nonlocal parameters

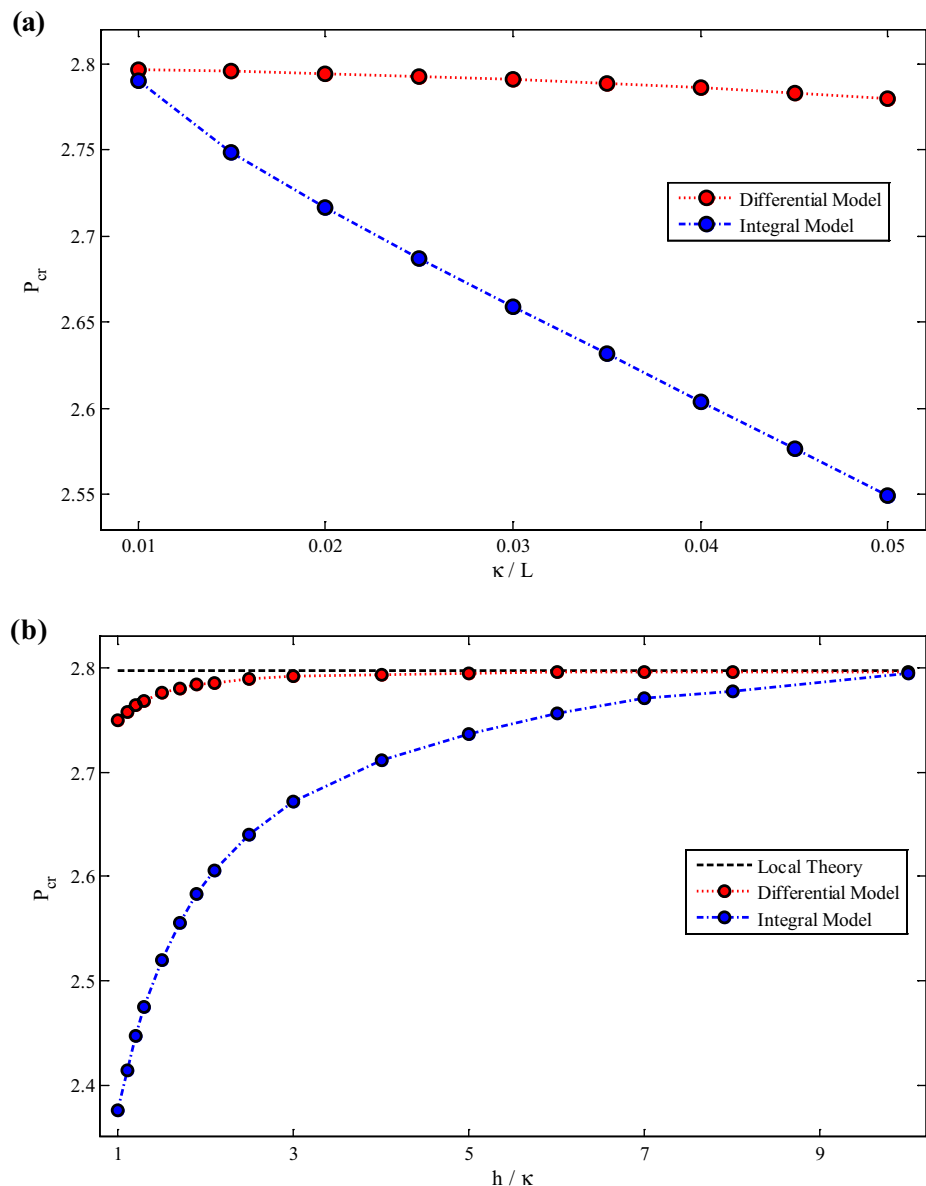
K		0.0	0.5	1.0	1.5	2.0
10	Ref [52]	1.2063	1.1989	1.1773	1.1431	1.0983
	Differential model	1.2063	1.1989	1.1772	1.1428	1.0979
	Integral model	–	1.0997	0.9884	0.8874	0.7971
12	Ref [52]	0.8387	0.8352	0.8246	0.8077	0.7851
	Differential model	0.8387	0.8351	0.8246	0.8076	0.7849
	Integral model	–	0.7782	0.7123	0.6512	0.5953
14	Ref [52]	0.6167	0.6147	0.6090	0.5997	0.5872
	Differential model	0.6167	0.6147	0.6090	0.5997	0.5871
	Integral model	–	0.5793	0.5372	0.4976	0.4607
16	Ref [52]	0.4724	0.4712	0.4679	0.4623	0.4549
	Differential model	0.4724	0.4712	0.4679	0.4623	0.4548
	Integral model	–	0.4480	0.4194	0.3923	0.3668
18	Ref [52]	0.3734	0.3726	0.3705	0.3670	0.3623
	Differential model	0.3734	0.3726	0.3705	0.3671	0.3623
	Integral model	–	0.3567	0.3365	0.3171	0.2987
20	Ref [52]	0.3025	0.3020	0.3006	0.2984	0.2952
	Differential model	0.3025	0.3020	0.3006	0.2983	0.2952
	Integral model	–	0.2907	0.2758	0.2616	0.2479

by which one can find that the absolute values of convergence errors in cases of $\kappa/L = 0.01$, $\kappa/L = 0.02$, and $\kappa/L = 0.03$ of integral model are, respectively, equal to 0.230, 0.132, and 0.071 percent, indicating the desirable rate of convergence. Accordingly, for the rest of paper, $n = 26$ and $n = 10$ are chosen for the analysis of integral and differential models, respectively.

To verify the accuracy of presented formulation and solution methodology for both integral and differential forms of nonlocal elasticity, a comparison is made with Ref [52] and corresponding results are tabulated in Table 1. Wang et al. [52] studied the buckling characteristics of nano-rods on the basis of the Timoshenko beam model and differential formulation of nonlocal elasticity. Since there are no size-dependent investigations on the

buckling problem based on the integral model, only the differential model of present study can be validated. However, the results of integral model of present approach are given for comparison purpose. Considered material and geometrical data are: $E = 1\text{TPa}$ and $\nu = 0.19$, and rod diameter $d = 1\text{nm}$. It should be noted that in Ref. [52], the shear constitutive equation is the same as that in the classical theory, and the normal constitutive relation is considered to be $(1 - \kappa^2 \nabla^2) \sigma_{xx} = E \varepsilon_{xx}$. By neglecting the first item and for comparison purpose, the elastic matrix \mathbf{C} is reformulated as $\lambda + 2\mu \rightarrow E$. Accordingly, it is seen that responses of differential model are in excellent agreement with those of Ref [52]. In addition, the trend of changes is identical in case of the proposed integral model. As it will be more highlighted in the following, the obtained results of integral model of

Fig. 2 Variations of dimensionless critical buckling load of clamped-free nanobeam with **a** nonlocal parameter-to-length and **b** thickness-to-nonlocal parameter ratios



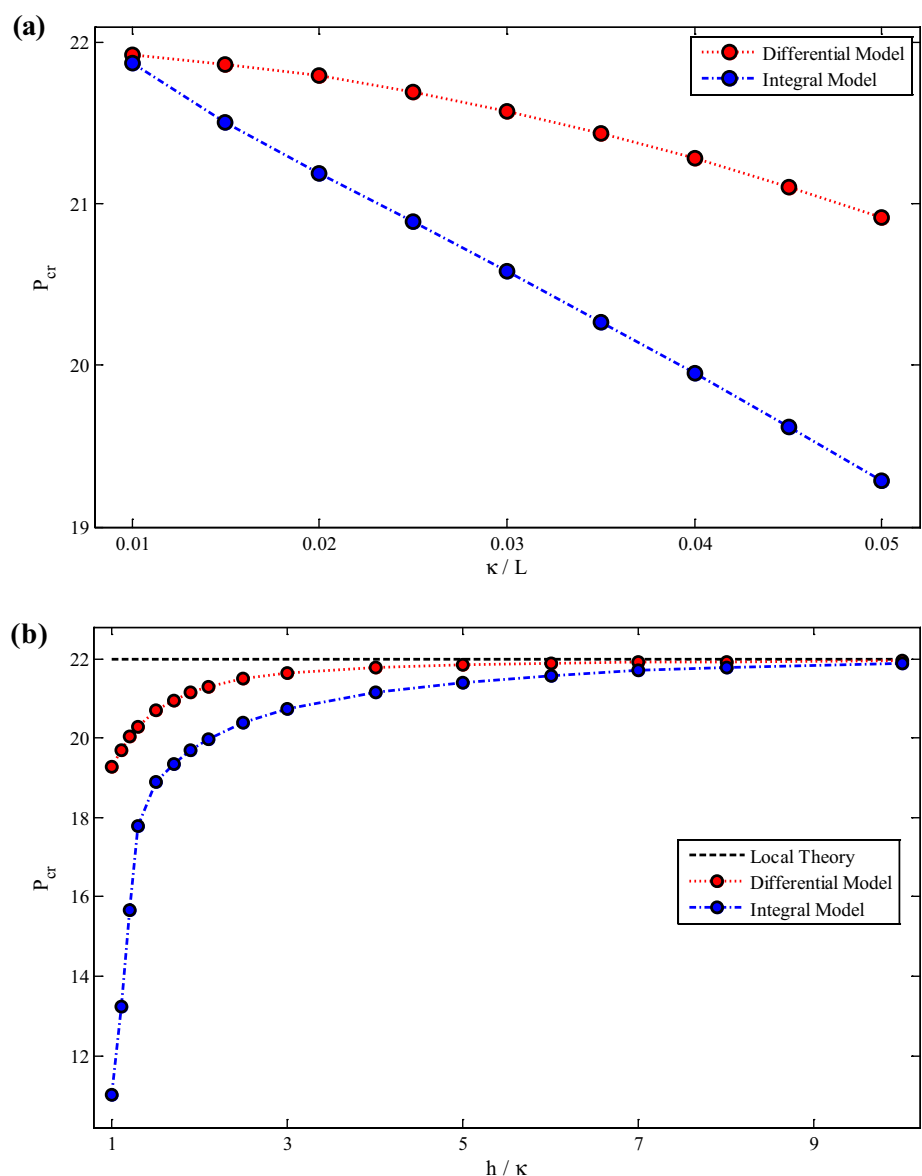
nonlocal continuum are smaller than those of the differential model. This is due to the fact that these models do not necessarily represent the same formulations [39–47]. The differential model is devised based on the Green function assumption of the specific group of kernel functions in the original integral model [20].

In Figs. 2, 3, and 4, the dimensionless critical buckling load of nanobeams with different end conditions is plotted versus nonlocal parameter-to-length ratio (κ/L) with considering $h = 1\text{nm}$, and versus the thickness-to-nonlocal parameter ratio (h/κ) with considering $\kappa = 0.1\text{nm}$. The results of these figures are generated using integral and differential nonlocal models. In addition, to better show the nonlocal effect, the classical results (corresponding to

$\kappa = 0$ in differential model of nonlocal elasticity) are given in Figs. 2, 3, and 4b.

Figures 2, 3, 4a indicate that as the nonlocal parameter-to-length ratio gets larger, the critical buckling loads obtained from both the integral and differential models decrease. However, the results of integral model are more affected by increasing κ/L . In addition, Figs. 2, 3, 4b show that at a given thickness-to-nonlocal parameter ratio, the critical buckling load obtained based on the integral model is smaller than that based on the differential model. It is seen that the difference between the predictions of two models has the maximum value at $h/\kappa = 1$, and the results of both models tend to the classical results by increasing h/κ .

Fig. 3 Variations of dimensionless critical buckling load of clamped-simply supported nanobeam with **a** nonlocal parameter-to-length and **b** thickness-to-nonlocal parameter ratios



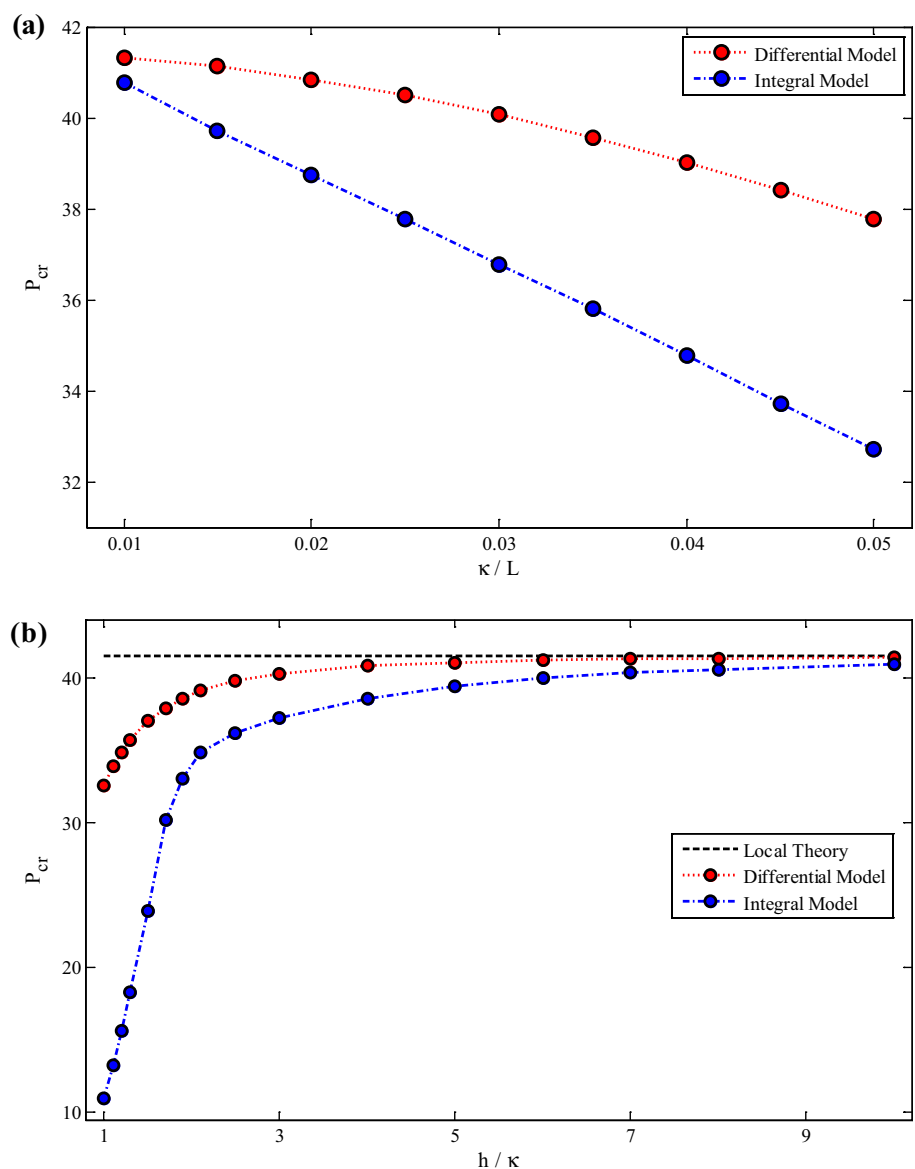
From the presented results, one can find that there is no paradox in the results of differential nonlocal model for the buckling problem as reported in [52, 53].

5 Conclusion

The buckling behavior of Timoshenko nanobeams subject to various types of boundary conditions was investigated in this article based on an isogeometric analysis. The small-scale effect was taken into account using both differential and integral models of Eringen’s nonlocal elasticity theory. The governing equations were derived in the vector–matrix representation which can be easily

used in the isogeometric analysis. The effects of nonlocal parameter-to-length and thickness-to-nonlocal parameter ratios on the critical buckling loads of nanobeams were illustrated. It was shown that the effect of nonlocal parameter is the same in both differential and integral models, i.e., using the differential nonlocal model does not lead to paradoxical results (increasing the buckling load with increasing the nonlocal parameter). However, there are considerable differences between the values of critical buckling loads predicted by the two models. This reveals that the results of differential model are not necessarily identical to the ones obtained based on the original integral model of Eringen’s theory for the buckling analysis of nanobeams.

Fig. 4 Variations of dimensionless critical buckling load of clamped–clamped nanobeam with **a** nonlocal parameter-to-length and **b** thickness-to-nonlocal parameter ratios



References

- M.E. Gurtin, A.I. Murdoch, A continuum theory of elastic material surfaces. *Arch. Rat. Mech. Anal.* **57**, 291–323 (1975)
- M.E. Gurtin, A.I. Murdoch, Surface stress in solids. *Int. J. Solids Struct.* **14**, 431–440 (1978)
- P. Lu, L.H. He, H.P. Lee, C. Lu, Thin plate theory including surface effects. *Int. J. Solids Struct.* **43**, 4631–4647 (2006)
- C.Q. Ru, A strain-consistent elastic plate model with surface elasticity. *Continuum Mech. Thermodyn.* **28**, 263–273 (2015)
- H. Rouhi, R. Ansari, M. Darvizeh, Nonlinear free vibration analysis of cylindrical nanoshells based on the Ru model accounting for surface stress effect. *Int. J. Mech. Sci.* **113**, 1–9 (2016)
- R. Ansari, A. Norouzzadeh, R. Gholami, M. Faghieh Shojaei, M.A. Darabi, Geometrically nonlinear free vibration and instability of fluid-conveying nanoscale pipes including surface stress effects. *Microfluid. Nanofluid.* **20**, 1–14 (2016)
- H. Rouhi, R. Ansari, M. Darvizeh, Size-dependent free vibration analysis of nanoshells based on the surface stress elasticity. *Appl. Math. Model.* **40**, 3128–3140 (2016)
- R.D. Mindlin, Second gradient of strain and surface tension in linear elasticity. *Int. J. Solids Struct.* **1**, 417–438 (1965)
- D.C.C. Lam, F. Yang, A.C.M. Chong, J. Wang, P. Tong, Experiments and theory in strain gradient elasticity. *J. Mech. Phys. Solids* **51**, 1477–1508 (2003)
- K.A. Lazopoulos, On bending of strain gradient elastic microplates. *Mech. Res. Commun.* **36**, 777–783 (2009)
- R.D. Mindlin, H.F. Tiersten, Effects of couple-stresses in linear elasticity. *Arch. Ration. Mech. Anal.* **11**, 415–448 (1962)
- W.T. Koiter, Couple stresses in the theory of elasticity. *Proc. Koninklijke Nederlandse Akademie van Wetenschappen (B)* **67**, 17–44 (1964)
- G.C. Tsiatas, A new Kirchhoff plate model based on a modified couple stress theory. *Int. J. Solids Struct.* **46**, 2757–2764 (2009)
- M. Shaat, A. Abdelkefi, Modeling the material structure and couple stress effects of nanocrystalline silicon beams for pull-in and bio-mass sensing applications. *Int. J. Mech. Sci.* **101–102**, 280–291 (2015)
- E. Kröner, Elasticity theory of materials with long range cohesive forces. *Int. J. Solids Struct.* **3**, 731–742 (1967)
- J. Krumhansl, in *Some Considerations of the Relation Between Solid State Physics and Generalized Continuum Mechanics*, ed. by E. Kröner, *Mechanics of Generalized Continua. IUTAM Symposia.* (Springer, Berlin Heidelberg, 1968), pp. 298–311
- I.A. Kunin, in *The Theory of Elastic Media with Microstructure and the Theory of Dislocations*, ed. by E. Kröner, *Mechanics of Generalized Continua. IUTAM Symposia.* (Springer, Berlin Heidelberg, 1968), pp. 321–329
- A.C. Eringen, Nonlocal polar elastic continua. *Int. J. Eng. Sci.* **10**, 1–16 (1972)
- A.C. Eringen, D.G.B. Edelen, On nonlocal elasticity. *Int. J. Eng. Sci.* **10**, 233–248 (1972)
- A.C. Eringen, On differential equations of nonlocal elasticity and solutions of screw dislocation and surface waves. *J. Appl. Phys.* **54**, 4703–4710 (1983)
- H.T. Thai, T.P. Vo, A nonlocal sinusoidal shear deformation beam theory with application to bending, buckling, and vibration of nanobeams. *Int. J. Eng. Sci.* **54**, 58–66 (2012)
- Y. Lei, T. Murmu, S. Adhikari, M.I. Friswell, Dynamic characteristics of damped viscoelastic nonlocal euler-bernoulli beams. *Eur. J. Mech. A/Solids* **42**, 125–136 (2013)
- S. Seifoori, G.H. Liaghat, Low velocity impact of a nanoparticle on nanobeams by using a nonlocal elasticity model and explicit finite element modeling. *Int. J. Mech. Sci.* **69**, 85–93 (2013)
- R. Ansari, R. Gholami, H. Rouhi, Size-dependent nonlinear forced vibration analysis of magneto-electro-thermo-elastic Timoshenko nanobeams based upon the nonlocal elasticity theory. *Compos. Struct.* **126**, 216–226 (2015)
- R. Ansari, J. Torabi, Numerical study on the free vibration of carbon nanocones resting on elastic foundation using nonlocal shell model. *Appl. Phys. A* **122**, 1073 (2016)
- R. Li, G.A. Kardomateas, Vibration characteristics of multi-walled carbon nanotubes embedded in elastic media by a nonlocal elastic shell model. *J. Appl. Mech.* **74**, 1087–1094 (2007)
- R. Ansari, A. Shahabodini, H. Rouhi, A. Alipour, Thermal buckling analysis of multi-walled carbon nanotubes through a nonlocal shell theory incorporating interatomic potentials. *J. Therm. Stresses* **36**, 56–70 (2013)
- K. Kiani, Vibration behavior of simply supported inclined single-walled carbon nanotubes conveying viscous fluids flow using nonlocal rayleigh beam model. *Appl. Math. Model.* **37**, 1836–1850 (2013)
- R. Ansari, H. Rouhi, S. Sahmani, Calibration of the analytical nonlocal shell model for vibrations of double-walled carbon nanotubes with arbitrary boundary conditions using molecular dynamics. *Int. J. Mech. Sci.* **53**, 786–792 (2011)
- S. Dastjerdi, M. Jabbarzadeh, Nonlinear bending analysis of bilayer orthotropic graphene sheets resting on Winkler–Pasternak elastic foundation based on non-local continuum mechanics. *Compos. Part B Eng.* **87**, 161–175 (2016)
- R. Ansari, A. Norouzzadeh, Nonlocal and surface effects on the buckling behavior of functionally graded nanoplates: An isogeometric analysis. *Physica E* **84**, 84–97 (2016)
- H. Kananipour, Static analysis of nanoplates based on the nonlocal Kirchhoff and Mindlin plate theories using DQM. *Lat. Am. J. Solids Struct.* (2014). doi:[10.1590/S1679-78252014001000001](https://doi.org/10.1590/S1679-78252014001000001).
- R. Ansari, A. Shahabodini, H. Rouhi, A nonlocal plate model incorporating interatomic potentials for vibrations of graphene with arbitrary edge conditions. *Curr. Appl. Phys.* **15**, 1062–1069 (2015)
- L.L. Zhang, J.X. Liu, X.Q. Fang, G.Q. Nie, Effects of surface piezoelectricity and nonlocal scale on wave propagation in piezoelectric nanoplates. *Eur. J. Mech. A/Solids* **46**, 22–29 (2014)
- R. Ansari, A. Shahabodini, H. Rouhi, Prediction of the biaxial buckling and vibration behavior of graphene via a nonlocal atomistic-based plate theory. *Compos. Struct.* **95**, 88–94 (2013)
- H. Rouhi, R. Ansari, Nonlocal analytical Flugge shell model for axial buckling of double-walled carbon nanotubes with different end conditions. *NANO* **7**, 1250018 (2012)
- H.S. Shen, Y.M. Xu, C.L. Zhang, Prediction of nonlinear vibration of Bilayer Graphene sheets in thermal environments via molecular dynamics simulations and nonlocal elasticity. *Comput. Meth. Appl. Mech. Eng.* **267**, 458–470 (2013)
- Y. Liang, Q. Han, Prediction of the nonlocal scaling parameter for Graphene sheet. *Eur. J. Mech. A/Solids* **45**, 153–160 (2014)
- J. Peddieson, G.R. Buchanan, R.P. McNitt, Application of nonlocal continuum models to nanotechnology. *Int. J. Eng. Sci.* **41**, 305–312 (2003)
- Q. Wang, K.M. Liew, Application of nonlocal continuum mechanics to static analysis of micro-and nano-structures. *Phys. Lett. A* **363**, 236–242 (2007)
- C. Polizzotto, Nonlocal elasticity and related variational principles. *Int. J. Solids Struct.* **38**, 7359–7380 (2001)
- A.A. Pisano, P. Fuschi, Closed form solution for a nonlocal elastic bar in tension. *Int. J. Solids Struct.* **40**, 13–23 (2003)
- N. Challamel, C. Wang, The small length scale effect for a nonlocal cantilever beam: a paradox solved. *Nanotechnology* **19**, 345703 (2008)

44. N. Challamel, L. Rakotomanana, L. Le Marrec, A dispersive wave equation using nonlocal elasticity. *Comptes Rendus Mécanique* **337**, 591–595 (2009)
45. P. Khodabakhshi, J.N. Reddy, A unified integro-differential nonlocal model. *Int. J. Eng. Sci.* **95**, 60–75 (2015)
46. J. Fernández-Sáez, R. Zaera, J. Loya, J.N. Reddy, Bending of Euler–Bernoulli beams using Eringen’s integral formulation: A paradox resolved. *Int. J. Eng. Sci.* **99**, 107–116 (2016)
47. A. Norouzzadeh, R. Ansari, Finite element analysis of nano-scale Timoshenko beams using the integral model of nonlocal elasticity. *Physica E* **88**, 194–200 (2017)
48. T.J. Hughes, J.A. Cottrell, Y. Bazilevs, Isogeometric analysis: CAD, finite elements, NURBS, exact geometry and mesh refinement. *Comput. Meth. Appl. Mech. Eng.* **194**, 4135–4195 (2005)
49. J.A. Cottrell, T.J. Hughes, Y. Bazilevs, *Isogeometric Analysis: Toward Integration of CAD and FEA*. (Wiley, New Jersey, 2009)
50. H. Ersoy, K. Mercan, Ö Civatek, Frequencies of FGM shells and annular plates by the methods of discrete singular convolution and differential quadrature methods. *Compos. Struct.* (2016). [10.1016/j.compstruct.2016.11.051](https://doi.org/10.1016/j.compstruct.2016.11.051)
51. Ö. Civatek, Discrete singular convolution method for the free vibration analysis of rotating shells with different material properties. *Compos. Struct.* **160**, 267–279 (2017)
52. C.M. Wang, Y.Y. Zhang, S.S. Ramesh, S. Kitipornchai, Buckling analysis of micro- and nano-rods/tubes based on nonlocal Timoshenko beam theory. *J. Phys. D Appl. Phys.* **39**, 3904–3909 (2006)
53. N. Challamel, Z. Zhang, C.M. Wang, J.N. Reddy, Q. Wang, T. Michelitsch, B. Collet, On nonconservativeness of Eringen’s nonlocal elasticity in beam mechanics: correction from a discrete-based approach. *Arch. Appl. Mech.* **84**, 1275–1292 (2014)